

In the following there are two retrieval algorithms. The first one is the Shack-Hartmann wavefront correction method (SH-algorithm), which is commonly used to reconstruct random phase distortions caused by the aberrations [19,20]. Its principle is based on the measurement of local slopes incoming to the Hartmann mask wavefront. The mask wavefronts are mathematical functions called Zernike polynomials. Any wavefront $\varphi(x, y)$ can completely be described by a linear combination of Zernike polynomials Z_0, Z_1, \dots, Z_N [19]

$$\varphi(x, y) = \sum_{k=0}^N a_k Z_k(x, y). \quad (5)$$

Now, assuming that $\varphi(x, y)$ is the deformation wavefront caused by turbulent aberrations. By model estimation and using the least-squares method, the coefficients a_i can be obtained by solving the equation

$$\varphi'_x(x, y) = \sum_{k=1}^N a_k Z_{kx}(x, y), \quad (6)$$

and

$$\varphi'_y(x, y) = \sum_{k=0}^N a_k Z_{ky}(x, y). \quad (7)$$

that is

$$\begin{pmatrix} G_x(1) \\ G_y(1) \\ \vdots \\ G_x(m) \\ G_y(m) \end{pmatrix} = \begin{pmatrix} D_{1x}(1) & \cdots & D_{nx}(1) \\ D_{1y}(1) & \cdots & D_{ny}(1) \\ \vdots & \cdots & \vdots \\ D_{1x}(m) & \cdots & D_{nx}(m) \\ D_{1y}(m) & \cdots & D_{ny}(m) \end{pmatrix} \begin{pmatrix} a_1 \\ \vdots \\ a_n \end{pmatrix}.$$

where, $G_x(m) = \varphi'_x(m)$, $G_y(m) = \varphi'_y(m)$, $D_{kx}(m) = Z_{kx}(m)$, and $D_{ky}(m) = Z_{ky}(m)$. This equation can be expressed in a simplified form

$$G = DA, \quad (8)$$

and the coefficients of Zernike polynomial A is can then be calculated by

$$A = D^{-1}G. \quad (9)$$

This way, we could get the phase of deformation wavefront caused by atmosphere turbulence using above coefficients and Eq. (5).

The second retrieval algorithm is a phase correction method for OAM states, which is proposed to measure and correct the surface defects of beam by using Gerchberg-Saxton phase retrieval algorithm (GS-algorithm) [21]. GS-algorithm will deal there with the problem of finding the phase $\varphi(x, y)$ of a light field by just determining the modulus $A(k_x, k_y)$ of its Fourier transform as

$$A(k_x, k_y) \exp[i\Phi(k_x, k_y)] = F\{\exp[i\varphi(x, y)]\}. \quad (10)$$

In [21], $\varphi(x, y)$ corresponds to the hologram function, and $A(k_x, k_y)$ to the amplitude of the observed doughnut mode. GS-algorithm is iterative, and its procedure is as follows. A perfect phase spiral is used as a starting point, and the illumination beam profile is selected as the magnitude in the Spatial Light Modulation plane. A complex Fast Fourier Transform (FFT) is used to generate the phase in the diffraction plane. The magnitude part of a perfect ring is discarded and replaced with the distorted image generated by the SLM, and then transformed back to the SLM plane, where the magnitude is replaced with the illumination beam profile. After a few iterations of the loop, the phase will generally converge to a value, and the phase of the aberration can be retrieved. Moreover, it is shown that this retrieval algorithm can be implemented by experiment [22].

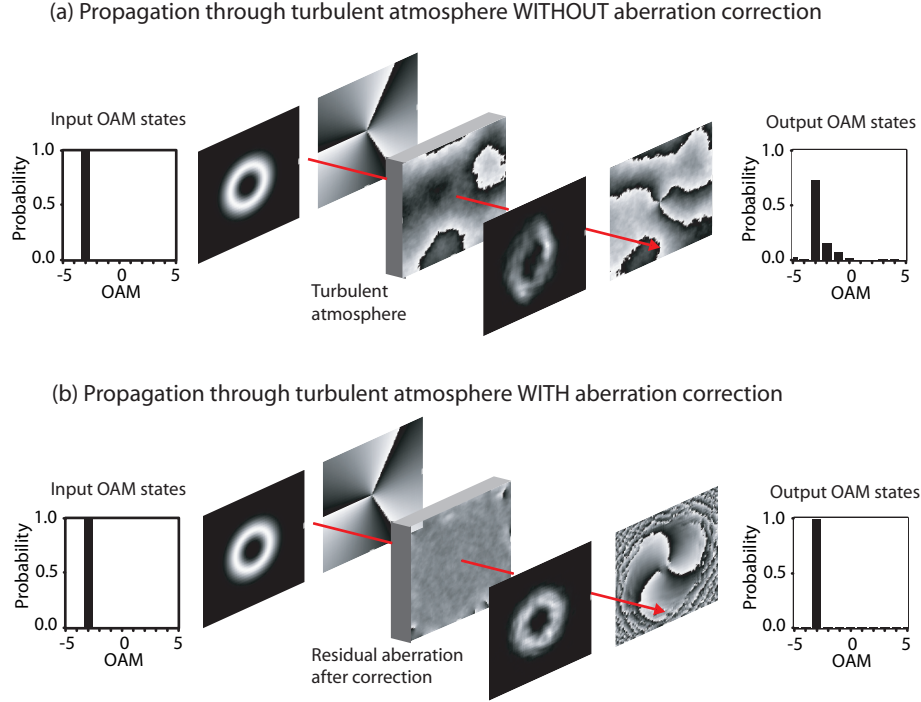


Fig. 1. The aberration caused by atmosphere turbulence and the mitigation effect of the aberration correction methods. (a) propagation through turbulent atmosphere without aberration correction (b) propagation through turbulent atmosphere with aberration correction.

3. Simulation results

In this section, we will verify the mitigation effect of both correction methods by numerical simulations. We discuss the cases with a single OAM state propagating through turbulence and a communication link caused by the atmosphere turbulence.

3.1. A single OAM state propagating through turbulence and its purity

Fig. 1 shows the aberration caused by the atmosphere turbulence and a single OAM state propagating through turbulent atmosphere with and without aberration correction. The parameters for the simulation of atmosphere turbulence are the following: $C_n^2 = 5 \times 10^{-13} \text{m}^{-2/3}$, $L_0 = 50\text{m}$, $l_0 = 0.0002\text{m}$, $N = 140$, $\Delta x = 0.0003\text{m}$, and $\Delta Z = 50\text{m}$. In the simulation, there are supposed five phase screens during the beam propagation. The results show that the purity of the input OAM state, $l = -3\hbar$, is damaged by the turbulent atmosphere, and the OAM state can be recovered by an aberration correction method.

In order to express the damaged effect of atmosphere turbulence and the recovery impact of aberration correction, we use decomposition in Fig. 1. Since LG modes are an orthogonal set of functions, they will compose a complete basis. Any state can be decomposed using this orthogonal basis, which is

$$\Psi(r, \theta, z) = \sum_p \sum_l a_{p,l}(z) LG_{p,l}(r, \theta). \quad (11)$$

The probability of obtaining a measurement, $l_z = \ell\hbar$, is obtained by summing all probabilities

associated with that eigenvalue

$$P(l) = \sum_p |a_{p,l}(z)|^2, \quad (12)$$

where the superposition coefficients $a_{p,l}(z)$ are given by the inner products

$$a_{p,l}(z) = \langle LG_{p,l}(r, \theta) | \Psi(r, \theta, z) \rangle. \quad (13)$$

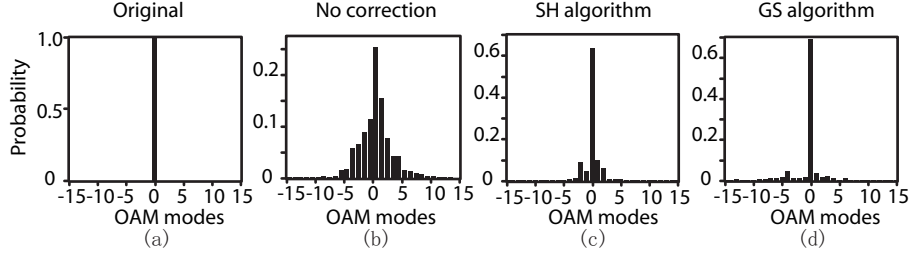


Fig. 2. Decomposition of the beam after passing through atmospheric turbulence with and without a correction. (a) original decomposition (b) without a correction (c) corrected by the Shark-Hartmann wavefront correction method (d) corrected by the phase correction method for OAM states.

In order to compare the mitigation effect of SH-algorithm and GS-algorithm presented in section 2, Fig. 2 shows the decomposition of the received state with the two correction methods in strong aberration case. The results show that for OAM $\ell=0$ state, the probability of the OAM state keeping on $\ell=0$ is only 25.3% in the atmospheric turbulence environment with $C_n^2 = 1 \times 10^{-12} \text{m}^{-2/3}$, $L_0 = 50\text{m}$, $l_0 = 0.0002\text{m}$, $N = 128$, $\Delta x = 0.0003\text{m}$, $\Delta Z = 100\text{m}$. This probability can be improved to 63.8% by using SH-algorithm, where 12th order of Zernike polynomials have been used to estimate the wavefront. And this probability can be enhanced to 69% by using GS-algorithm. The results show that the two aberration correction methods have improved the beam quality significantly, then the phase correction method for OAM states show a better performance.

3.2. A communication system on OAM and its capacity

As discussed above, it is known that a single LG mode state will be polluted by turbulent aberration when it passes through atmospheric turbulence in free space. For a communication link based on OAM, turbulent aberrations may cause noise to the original OAM state. It is important to estimate the probability of keeping the original state in this communication channel [8–10].

Fig. 3 shows that the probability of keeping original OAM state varies with the strength of turbulent aberration. The results show that the probability of obtaining the original LG mode (corresponding to $\Delta = 0$) decreases as C_n^2 increases. At the same time, the probability for shifting to adjacent one LG mode ($\Delta = \pm 1$) is higher than those to shift to two ($\Delta = \pm 2$) or more modes. As the adjacent azimuthal modes increase, the probabilities of obtaining the original LG modes ($\Delta \neq 0$) decrease significantly.

Generally, channel capacity is regarded as a quality of a communication system. The noise caused by atmosphere turbulence can be described by a channel matrix $H = [H_{mm}]$, where the conditional probabilities H_{mm} can be evaluated by Eqs. (12) and (13). Here, m is the number of transmitted OAM states and n is the number of received states. For the simplicity, we select $\ell_m = 0, 1$ as the transmitted OAM states for $L = 1$ and the received OAM states are selected

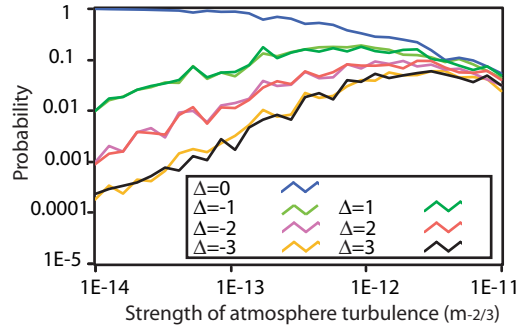


Fig. 3. The effect of turbulence on the propagating OAM quantum states as functions of C_n^2 , where C_n^2 varies from $1 \times 10^{-14} \text{m}^{-2/3}$ to $1 \times 10^{-11} \text{m}^{-2/3}$, representing the strength of turbulent aberration changing from weak to strong. The distance of propagating is 100m, the outer scale is 50m, and the inner scale is 0.0002m. The simulation grid comprises 128×128 elements, and the grid spacing size is 0.0003m.

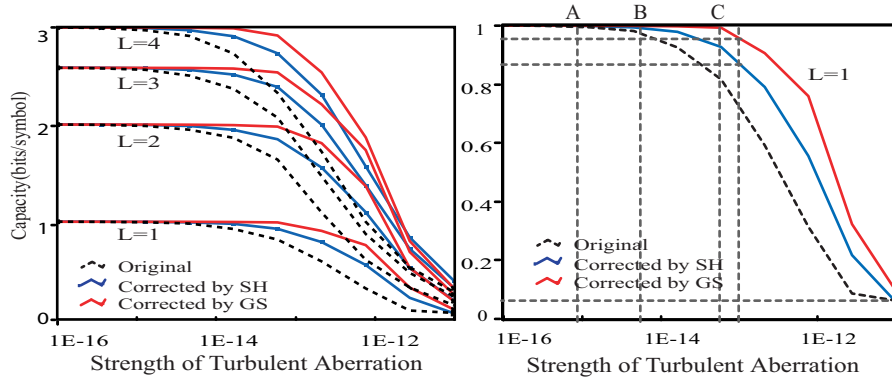


Fig. 4. Comparison of the channel capacity for a communication link employing OAM states of single photon through atmospheric turbulence, corrected by Shark-Hartmann wavefront correction method and the phase correction method for OAM states.

from $\ell_n = -15$ to $\ell_n = 15$. Similarly, we will select $\ell_m = 0, 1, 2, 3$ for $L = 2$ and decompose the received state from $\ell_n = -15$ to $\ell_n = 15$. We use the same scheme for $L = 3$ and $L = 4$. After we obtain the channel matrix, we can calculate the capacity of this discrete channel by the Blahut-Arimoto algorithm [23]. Fig. 4 shows the channel capacities for communication systems using different LG modes propagating through atmospheric turbulence with and without the two correction methods. The results show that the channel capacities decrease rapidly as C_n^2 increase, and both the correction methods can improve the channel capacities effectively. For example, atmosphere turbulence causes the capacity of two input OAM states ($L = 1$) to decrease from 1 bits/symbol to 0.08 bits/symbol when the structure constant of the index refraction varies from $1 \times 10^{-16} \text{m}^{-2/3}$ to $1 \times 10^{-11} \text{m}^{-2/3}$. The decreasing point A means atmosphere turbulence will cause noise to the communication channel at $C_n^2 = 9 \times 10^{-16} \text{m}^{-2/3}$. SH-algorithm has postponed this decreasing to point B, where $C_n^2 = 7.5 \times 10^{-15} \text{m}^{-2/3}$, and GS-algorithm has changed to $C_n^2 = 7 \times 10^{-14} \text{m}^{-2/3}$ (point C). In other words, the capacity of the communication

channel will be improved by both the correction methods. For $L = 1$ and $C_n^2 = 1 \times 10^{-13} \text{m}^{-2/3}$ (a slight strong turbulent atmosphere), the capacity of a communication link in Fig. 4 is 0.725 bit/symbol. At this case, SH-algorithm has improved the capacity to 20.1% (0.875 bits/symbol), while GS-algorithm has enhanced this value to 0.96 bits/symbol (33%). Both correction methods have improved the purity of a single OAM state, and the capacity of a communication system on the OAM state significantly. Moreover, the phase correction method for OAM states is more effective for mitigating the turbulent aberrations.

4. Experimental results

From the above section, we find that the phase correction method for OAM states is more useful to overcome turbulent aberration in numerical simulations. On the other hand, if we use the observed intensity pattern in CCD as the deformation wavefront caused by turbulent aberration to Gerchberg-Saxton algorithm [22], the phase correction method for OAM states can be implemented experimentally. Therefore, we will discuss the effect of the phase correction method for OAM states as has been shown by the following experiments.

4.1. Experimental setup

Because LG modes of small helical charge have high sensitivity to the phase errors, even small phase irregularities cause significant deviations from their rotational symmetric 'doughnut' shape, we utilize $\ell = 1$ LG mode to determine the 'hologram' of the turbulent atmosphere aberration from the distorted shape of a focused doughnut mode. Unfortunately, this mode does not explain the change numerically. In order to illustrate the improvement of the phase correction method for OAM states to the turbulent aberration, we will design a referenced spot mode ($\ell = 0$) besides the doughnut, and we will use the participation function (also named as sharpness metric) to measure the spot quality. The participation function of the referenced spot is defined as following

$$P = \frac{(\sum_{i,j}^N I_{i,j})^2}{\sum_{i,j}^N I_{i,j}^2}, \quad (14)$$

where $I_{i,j}$ is the intensity of the $(i, j)^{th}$ pixel of the referenced spot. It is shown that the smaller value corresponds to the more tightly focused spot [24].

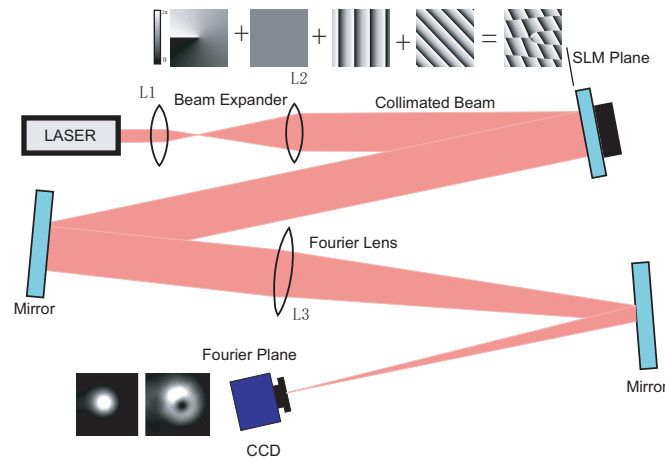


Fig. 5. The sketch of the experimental setup.

Fig. 5 shows the experimental system to test the turbulent aberration correction method. The reflective computer-controlled spatial light modulator shows a diffractive vortex lens, which transforms a collimated laser beam into an optical vortex of helical charge ℓ ($\ell = 1$ in the Fig. 5) and a referenced spot ($\ell = 0$) under somewhat turbulent aberration. As usual, the vortex lens is superposed by a grating in order to spatially separate the optical vortex generated in the first diffraction order from other orders. In order to detect the referenced spot besides the LG mode, different grating is assigned to LG mode and the referenced spot. The Fourier plane corresponds to the far-field diffraction pattern. A lens (L_3) is used to focus the image on CCD in the Fourier plane, and several mirrors are arranged so as to get the biggest image in CCD as possible.

4.2. improvement of the participation function

At first, we get a deformed doughnut and referenced spot when we include phase screen from the simulations about the turbulent aberration on the SLM, then we use the phase correction method for OAM states to obtain the "correction hologram" of the turbulent aberration, and add it on the SLM. Finally, we can get an improved doughnut and referenced spot in CCD. The participation function of the reference spot with and without the correction method show the improvement of the correction method. In order to calculate the participation function with and without the correction method, we divide the CCD into two interesting areas, one for showing the correction procedures ($\ell = 1$ LG mode), and one for participation function calculations ($\ell = 0$ LG mode).

According to the atmosphere turbulence model, the random phase screen caused by atmosphere turbulence is mainly determined by the constant of the index of refraction. In order to understand the mitigation effect of the correction method, we measure the participation function of referenced spot with and without the correction method. We let the index of refraction change while keeping the other simulation parameters be constant during the experiments. Since the phase screen caused by atmospheric turbulence is random, phase screen obtained from the simulation is different from time to time, even with the same simulation parameters. We give the average value of the participation function in each case over 20 values.

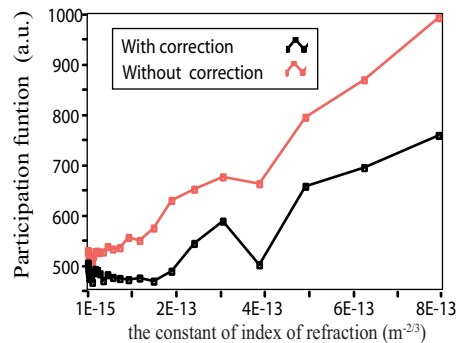


Fig. 6. The variance of the participation functions for the reference spot with the change of the index of refraction by the phase correction method for OAM states.

Fig. 6 shows the variances of participation function with the constant of index of refraction varying from 10^{-15} to 10^{-12} . The experimental results show that the values of participation function go down with the correction method, and the correction method is an effective way to mitigate the turbulent aberration. We get 45% maximum improvement and 17% average improvement by the change of strength of aberration.

5. Conclusion

In this work, we apply different aberration correction techniques [19, 21] to mitigate the deformation effect caused by the atmosphere turbulence. One is the Shack-Hartmann wavefront correction method, and the other is a phase correction method for OAM states. To quantify the improvements we calculate the channel capacities in a similar fashion to the method described in [8]. Our simulation results show that it is possible to recover the damaged LG mode caused by the atmosphere turbulence. The two correction methods have improved the purity of a single photon LG mode and the capacities of the free space optical communication channel produced by atmosphere turbulence significantly, and the phase correction method for OAM states outperforms the Shack-Hartmann wavefront correction method.

Using SLM, the phase correction method for OAM states is easier to implemented. We testify the correction method in a series of experiments. The experimental results show that the values of participation function decrease with the phase correction method for OAM states. The correction method is an effective way to mitigate the turbulent aberration both in simulations and experiments.

Acknowledgments

We would like to thank the anonymous referee for several useful comments. We are grateful to Prof. Jozef Gruska for careful reading the manuscript. Shengmei Zhao acknowledges support from the University Natural Science Research Foundation of JiangSu Province (11KJA510002), Foundation NJ210002, the project funded by the Priority Academic Program Development of Jiangsu Higher Education Institutions, and the open research fund of Key Lab of Broadband Wireless Communication and Sensor Network Technology (Ministry of Education), China. Longyan Gong acknowledges support from the national natural science foundation of China(No.10904074). The authors thank Optics group, School of Physics and Astronomy, Glasgow University for hosting Shengmei Zhao as a visitor while conducting this research.